Repeated segregation and energy dissipation in an axially segregated granular bed

2010 EPL 92 54004

(http://iopscience.iop.org/0295-5075/92/5/54004)

A Letters Journal Exploring the Frontiers of Physics

December 2010

EPL, **92** (2010) 54004
doi: 10.1209/0295-5075/92/54004

www.epljournal.org

Repeated segregation and energy dissipation in an axially segregated granular bed

M. M. H. D. Arntz[1], W. K. den Otter[2], H. H. Beeftink[1], R. M. Boom[1] and W. J. Briels[2(a)]

[1] *Food and Bioprocess Engineering Group, Wageningen University - P.O. Box 8129, 6700 EV Wageningen, The Netherlands, EU*
[2] *Computational Biophysics, Faculty of Science and Technology, University of Twente - P.O. Box 217, 7500 AE Enschede, The Netherlands, EU*

received 18 August 2010; accepted in final form 25 November 2010
published online 5 January 2011

PACS 45.70.Mg – Granular flow: mixing, segregation and stratification
PACS 02.70.Ns – Molecular dynamics and particle methods

Abstract – Discrete element simulations were used to study the segregation behaviour in a bed of bidisperse granules in a rotating drum. In the final state the large particles ended up in the upper part of the bed near the vertical walls. In order to arrive at this state, the system went through two cycles of structural changes, on top of which fast oscillations were observed between an axially segregated and a somewhat more mixed state. These oscillations were sustained by different angles of repose near the vertical walls and in the middle of the bed. Concomitantly with the structural changes, the system's energy dissipation went through two cycles after which it settled in the state requiring the least work of all traversed states, suggesting that the granular bed strives for minimal dissipation.

Understanding flow of granular matter is of great practical importance, since it occurs in many industrial processes at one stage or another. Flow of granular particles that are heterodisperse in size often results in mixing, but sometimes in segregation, of the various components. For example, an initially homogeneously mixed bidisperse bed of particles in a horizontal rotating drum in many cases segregates after only a few rotations, with the smaller particles generally accumulating in a submerged core spanning the entire length of the drum [1,2]. The boundary of this core performs erratic undulations with increasing amplitudes [2–4] until it reaches the outer surface and becomes visible as a sequence of bands of smaller particles separated by bands of larger particles [2–7]. On further rotation, the submerged connections between these bands break apart and the bed becomes axially segregated [8–10]. On very long time scales the bands generally diffuse and merge until ultimately only three bands [5], and sometimes only two bands [11], remain. The above description is a generic summary of many experimental findings, which sometimes may differ in their details. It has been confirmed by molecular dynamics simulations of dissipative grains with surface frictions by Taberlet *et al.* [4]. Detailed experimental investigations have been performed by Khan *et al.* [12].

Experiments on bidisperse rotating beds [7,9,13] indicate that end-wall effects can initiate band formation or determine the structure of the bands near the end-walls. In this paper, we report results of discrete element model (DEM) simulations of a drum with an aspect ratio of $L/D = 0.73$, with L being the length of the drum and D its diameter. This drum is small enough to be dominated by the presence of the end-walls, yet long enough to be called three dimensional. The rather small system size allows runs that are long enough to perform a detailed study of transient oscillations after the onset of rotation.

In order to analyse the results of our simulations we introduce three different types of order parameter, each of which gives information about the presence or absence of a different kind of structure. Together these order parameters allow a detailed monitoring of the evolution of the bed, and the end-wall effects in particular. Moreover we will calculate various contributions to the dissipation of energy and find that on the long run the system appears to strive for a state with minimal energy dissipation. This observation will be discussed at the appropriate point later in this paper.

In the discrete element model the particle positions, velocities and angular velocities are updated by means of a

(a) E-mail: w.j.briels@utwente.nl

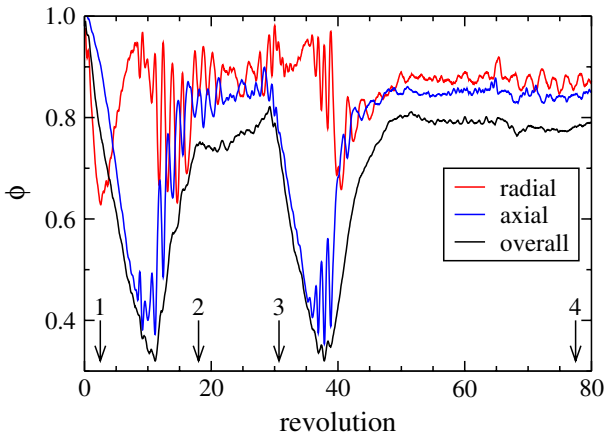

Fig. 1: (Colour on-line) Three order parameters plotted against the number of revolutions after onset of rotation of the drum: ϕ_r is low when radial segregation is pronounced, ϕ_a when axial segregation is pronounced, while ϕ_o quantifies the overall mixing state. All order parameters take values between 0 and 1, and have been smoothed by a running average over a quarter revolution to reduce the noise level. Snapshots of the system at the two deep minima are shown in fig. 2, snapshots at the four instances marked by arrows are shown in fig. 3.

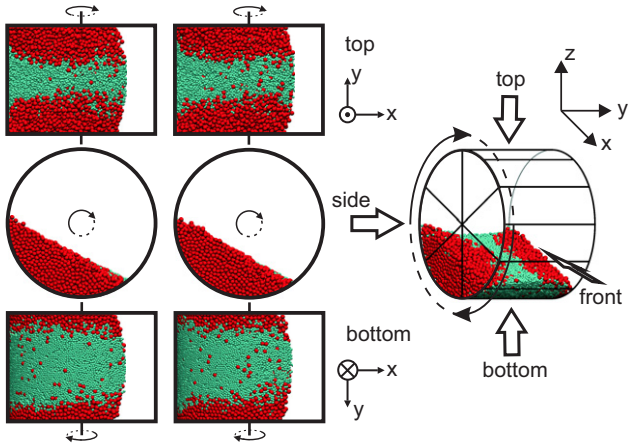

Fig. 2: (Colour on-line) Top, side and bottom views of the drum after 11 revolutions (left) and 38 revolutions (middle), corresponding to the two minima of the overall and axial order parameters in fig. 1. A three-dimensional view of the drum is presented on the right, with arrows indicating the various directions of view. The radius of the large particle (dark red) is twice that of the small particle (light green).

numerical integration of the classical equations of motion, given the contact forces exerted among neighbouring particles [14]. Forces between particles i and j are zero in case the corresponding width of the apparent overlap region Δ_{ij} is zero. Otherwise the normal force exerted on particle i by particle j is calculated as

$$\vec{F}_{ij}^{n} = -k_n \Delta_{ij} \hat{n}_{ij} - \eta_n \vec{v}_{ji}^{n}. \tag{1}$$

Here $\hat{n}_{ij}$ is the unit vector $\vec{r}_{ij}/r_{ij}$ with $\vec{r}_{ij} = \vec{r}_j - \vec{r}_i$ the position vector of particle j with respect to particle i and r_{ij} its length; $\vec{v}_{ij}$ is the velocity of particle j with respect to particle i and $\vec{v}_{ji}^{n}$ its component along $\hat{n}_{ij}$. Moreover, k_n is the elastic stiffness coefficient and η_n the normal damping coefficient. The latter is uniquely related to the so called restitution coefficient ϵ, which can easily be measured experimentally. The tangential force is calculated according to Schäfer's approximation of the Coulomb model [15], and is equal to

$$\vec{F}_{ij}^{t} = -\eta_t (\vec{v}_{ij}^{t} + (R_i \vec{\omega}_i - R_j \vec{\omega}_j) \times \hat{n}_{ij}) \tag{2}$$

or

$$\vec{F}_{ij}^{t} = -\mu F_{ij}^{n} \hat{t}_{ij}, \tag{3}$$

the actual force being the one with the smallest absolute value. Here $\vec{v}_{ij}^{t} = \vec{v}_{ij} - \vec{v}_{ij}^{n}$ and $\hat{t}_{ij} = \vec{v}_{ij}^{t}/v_{ij}^{t}$; R_i is the radius of particle i and $\vec{\omega}_i$ its angular velocity. Finally, η_t is the viscous friction coefficient and μ the Coulomb friction coefficient. Interactions between particles and the drum are similar to particle-particle interactions, but with distances and velocity differences calculated relative to the respective contact points with the walls. The cylindrical drum of diameter D and length L is oriented with its rotation axis along the y-axis and is closed by flat circular walls at both ends. The gravitational force points in the negative z-direction. The drum is characterized by its length $L = 220\,\mathrm{mm}$ and its diameter $D = 300\,\mathrm{mm}$. The particles have radii $R_1 = 2\,\mathrm{mm}$ and $R_2 = 4\,\mathrm{mm}$, respectively. When densely close packed, the particles occupy one fourth of the total volume of the drum, with eight times as many small particles as there are large particles. The drum is rotated with angular speed $\omega = \pi/2\,\mathrm{rad/s}$. The simulation parameters are: time step $\Delta t = 5 * 10^{-6}\,\mathrm{s}$, density of the particles $\rho = 2500\,\mathrm{kg/m^3}$, normal spring constant $k_n = 125\,\mathrm{N/m}$, normal friction coefficients are all calculated using a restitution coefficient of 0.1, tangential friction coefficient $\eta_t = 1.0\,\mathrm{kg/s}$, and Coulomb friction coefficient $\mu = 0.5$. We have carefully checked that the time step is small enough to guarantee conservation of energy during frictionless collisions.

We characterize the type and degree of segregation by a number of order parameters all deriving from the entropy of mixing [16] $S = \int \mathrm{d}^3 r \rho(\vec{r}) \sum_i x_i(\vec{r}) \ln x_i(\vec{r})$, normalized according to

$$\phi = \frac{S - S_{\mathrm{seg}}}{S_{\mathrm{mix}} - S_{\mathrm{seg}}}. \tag{4}$$

Here $\rho(\vec{r})$ is the particle density at $\vec{r}$ and $x_i(\vec{r})$ is the local number fraction of particles of type i. S_{seg} is the mixing entropy of the fully segregated system and S_{mix} that of the fully mixed system. Different order parameters are obtained by numerically calculating the integral using different grids. In all cases the grid was chosen such that each filled cell contained about 75 particles. In particular, ϕ_o corresponds to a grid of cubic cells, ϕ_r to a grid of bars along the drum axis, and ϕ_a to a grid of discs perpendicular to the drum axis. The subscripts indicate the type of information that is given by the particular

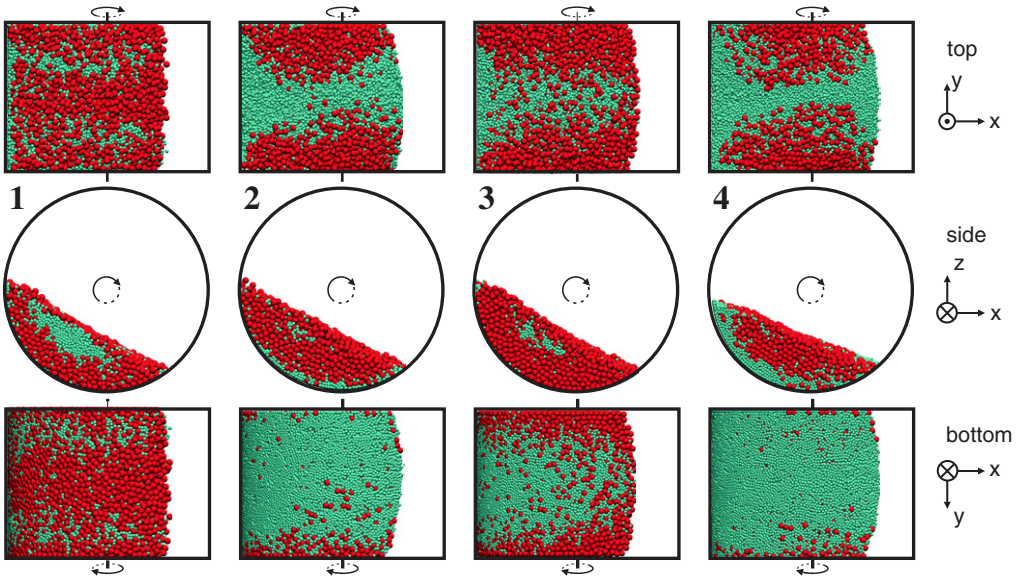

Fig. 3: (Colour on-line) Four sets of snapshots taken at increasing times corresponding with the arrows in fig. 1, showing top views (top), side views (center) and bottom views (bottom) of configurations with nearly identical overall order parameters. The first sets of snapshots is taken after 2.5 revolutions, when radial segregation is very pronounced. The second set is taken after 18 revolutions; after going through the ordered state displayed in fig. 2, most large particles have been removed from the bottom surface and put near the vertical walls —this state very much resembles the final stationary state shown on the right. Between the second and the final state, the system makes one more cycle through a sequence of states with low overall order parameter, illustrated in fig. 2, which starts after about 30 revolutions when the structure is like in the third snapshot.

order parameter. So, ϕ_o gives information about the overall mixing of the various components, ϕ_r is small in case of segregation along the radius of the drum and ϕ_a is small in case of segregation along the axis.

In the next few paragraphs we describe the structural changes that take place after the onset of rotation. In fig. 1 we have plotted the time development of all three order parameters during a simulation of 80 revolutions. The most striking features of this plot are the two minima of ϕ_o after 11 and 38 revolutions, respectively. In fig. 2 we have plotted top, bottom and side views of the drums at these points during the simulation. In both cases the drums are axially segregated with the smaller particles in the middle section and the larger particles near the end-walls. No small particles are visible in the side views, while only very few large particles are seen in the middle sections of the top and bottom views. Interestingly, there is a small asymmetry between the top and bottom views, in the sense that the middle section is slightly narrower in the top view than in the bottom view. The strong axial segregation in these two states is also signaled by minima in the corresponding axial order parameters.

We next discuss some of the details of fig. 1. Four points, all having approximately the same ϕ_o, have been marked on the horizontal axis, corresponding to the four snapshots in fig. 3. At the time of the first snapshot, after 2.5 revolutions, radial segregation is more or less complete, corroborated by the radial order parameter ϕ_r having a clear minimum at this instant. The top and bottom surfaces are well covered by large particles, while the small particles constitute the inner core of the drum, as is clear from the side view. From this time on, axial segregation sets in as indicated by a further decrease of ϕ_a, while radial segregation is temporarily blurred again, indicated by a rise of ϕ_r. After 11 rotations both ϕ_o and ϕ_a reach temporary minima, corresponding to pronounced axial segregation as discussed above. On continuation of the run, both ϕ_o and ϕ_a rise quickly until they reach a quasi-plateau where this rise becomes very slow. The second and third snapshots are taken at the beginning and end of this plateau. In the second snapshot (see fig. 3) the state of axial segregation (see fig. 2) has been destroyed to some extent and most of the large particles have been expelled from the bottom wall. At the end of the quasi-plateau the system has developed into a state which is partly radially segregated and partly axially segregated, shown in the third snapshot. This state is apparently rather unstable, since from here on the whole process more or less repeats itself. The system goes again through a state of axial segregation, see figs. 1 and 2, and next climbs again to some plateau with roughly constant order parameters. This time, hardly any developments occur on the plateau as is clear from the resemblance of the second and fourth snapshot in fig. 3, the latter being taken after 80 revolutions. We continued the run for another twenty revolutions and found no new developments. Moreover, similar mixing and demixing behaviour was observed in ten additional runs of 100 revolutions, each starting from

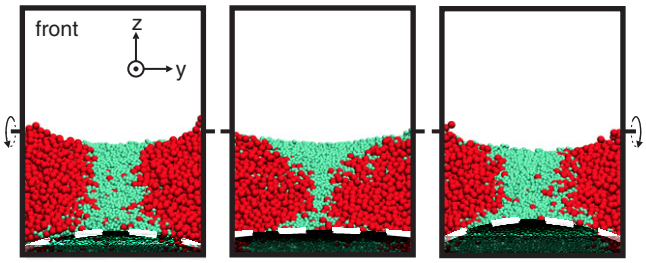

Fig. 4: (Colour on-line) Three consecutive front views at different phases of a fast oscillation. In the outer two snapshots the axial order parameter is small, while in the middle snapshot ϕ_a is large. In all snapshots the large particles are mostly near the vertical walls. In the left picture the angle of repose is larger near the vertical wall than in the middle of the drum, making the large particles roll inwards until halfway the upper surface and then outward again; this continues until in the middle snapshot the angle of repose has been equalized along the drum. Continuing rotation then builds up a new difference of angles of repose until this is maximal in the right snapshot. The dashed lines highlight the front contact lines of the bed and the cylindrical drum wall, separating the particles in contact with the wall (dark) from the particles at the surface of the bed (light). This line, like the rear contact line, bends and straightens during a fast oscillation.

a randomly mixed state, which all converged to the same final steady state.

We now concentrate on one more aspect of fig. 1. During the fast increases of ϕ_o and ϕ_a, oscillations with a period of about 1.5 revolutions are observed both in ϕ_a and in ϕ_r, but with opposite phases. These oscillations are absent in ϕ_o, indicating that the oscillations exchange axial for radial segregation without changing the overall segregation. A series of snapshots is shown in fig. 4, capturing the evolution of one single fast oscillation. When ϕ_a is maximal, the band of small particles in the middle of the drum is wide at the bottom and narrow at the free surface. In the minima of ϕ_a this difference has disappeared. These oscillations are different from the ones reported in the literature [8,17,18], where the widths of the small-particle bands at the surface vary by transport of particles through a radial core, while our system lacks such a core. The mechanism that sustains the observed fast oscillations can easily be understood. The reason is that the large particles, once they are driven to the periphery of the drum, have an angle of repose which is about four to six degrees larger than that of the small particles in the central part of the drum. As a result, on their way down at the surface of the bed, the large particles have a tendency to move inward, flooding the central part of the surface. For the same reason of having a somewhat larger angle of repose than the small particles, the tendency to move inward is reversed once the large particles have covered half their way down. The trajectories of the large particles at the surface of the bed are therefore very much as drawn in fig. 3 of Pohlman *et al.* [19]. The fast oscillations mentioned above occur because the large particles at the surface tend to move in large chunks being either at the upper surface or at the lower surface of the bed. When these chunks gradually disperse the oscillations disappear. It is worth mentioning that the dependence of the angle of repose on the position along the axis of the drum is not so much caused by the fact that it is the large particles which are at the periphery of the drum while the small particles are in the center, but rather is an effect caused by the end-walls themselves. Indeed, in additional simulations of monodisperse systems we found that both the small particles as well as the large particles had a somewhat larger angle of repose near the end-walls than in the center of the drum. The oscillations discussed above are therefore the single result of the presence of the end-walls. This conclusion was further corroborated by simulations of the bi-disperse system with periodic boundary conditions, in which case no oscillations occurred.

Until now we have described the structural changes that occur in the drum after the onset of rotation. The next obvious thing to do is to ask for a rule that governs the evolution just described. This question naturally consists of two parts, first, is there a final, stationary or periodic (or chaotic) state, and second, what principle governs the evolution from the initial to the final state? The latter of these questions is far beyond the scope of this paper. As to the former, we will only state a few observations done on our system. As is well known, stationary solutions of the Navier-Stokes equations neglecting the non-linear terms obey the principle of minimal dissipation [20,21]. A similar principle has been put forward by Glansdorff and Prigogine [22] to describe the occurrence of dissipative structures in non-equilibrium systems. We therefore have calculated the energy dissipation in our system after the onset of rotation, and will present our findings in the remaining part of this paper. For an extensive discussion of possible laws governing non-equilibrium structures we refer to a review paper by Martyushev and Seleznev [23] and some of the older literature [24–27]. Additional discussion may be found in the book of Öttinger [28].

In fig. 5 we show the time evolution of the total dissipation in the system and its various contributions. Obviously, on small time scales the dissipation fluctuates to some extent due to small displacements of the particles around some macroscopic state. As a result, in all references below to the various components of the total dissipation, averages over small time windows are implied. Moreover, it is perhaps worth mentioning that the dissipation that we discuss here is basically the dissipation of energy in the form of heat in the particles, and is not related to the changing structural entropy that we have used to define order parameters. First of all we notice that the total dissipation is about 25 percent smaller in the final stationary state than in the initial fully mixed state. From the various contributions to the dissipation on the long term we infer that it is mainly the lowering of the dissipation in the small particles that is responsible for

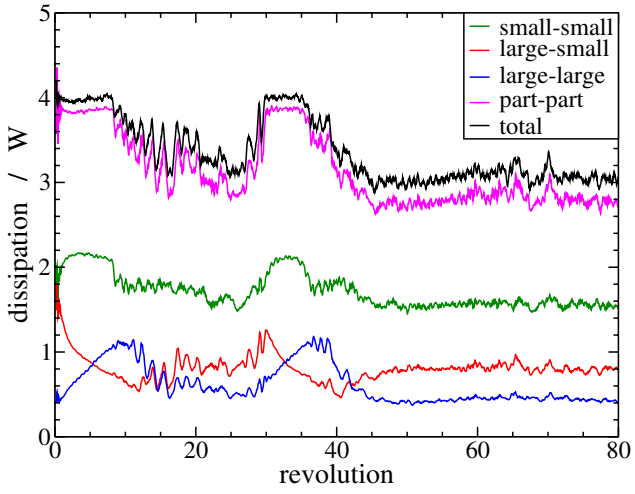

Fig. 5: (Colour on-line) Energy dissipation in units of watt as a function of the number of drum revolutions. During the early stage the total dissipation hardly changes, despite considerable changes in the individual contributions which reflect structural changes in the bed. Between revolutions 8 and 30 the total dissipation gradually relaxes to a quasi-stationary minimum. Near revolution number 30 the dissipation rises again just to go through the whole process again, to end in a final stationary state with an even lower energy dissipation rate than before the transition. The curves show running averages over a quarter revolution, to smoothen the noise on the instantaneous dissipation.

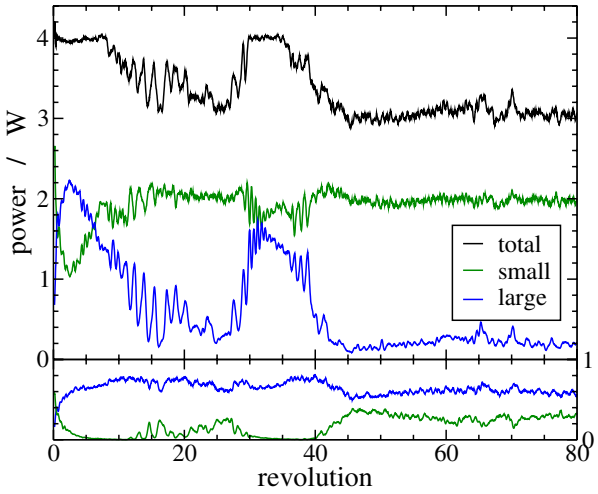

Fig. 6: (Colour on-line) Various contributions to the delivered power in units of watt as a function of the number of drum revolutions, with the upper and lower panel showing the power delivered at the cylindrical wall and the flat end-walls, respectively. Again the final state with minimal power consumption is arrived at via two cycles of similar evolution. It is seen that the dissipation is minimized by lowering the power transfer to the large particles. This is done by removing the large particles from contacts with the cylindrical walls. The natural fluctuations of the noise have been smoothed by employing running averages over a quarter revolution.

the overall decrease of dissipation. The dissipation due to collisions of the large particles among each other is almost the same in the final stationary state as in the initial mixed state. Dissipation due to small-small collisions decreases slightly with time, while the dissipation due to small-large collisions decreases most. This is in accordance with the observed segregation phenomena and lends credit to the principle of minimal dissipation as a selection criterion for the final stationary state. Short-lived fluctuations may momentarily raise or lower the dissipation, as seen in the graph, but the essence of the principle is that the long-term average tends to be minimal in the final state. Since the dissipation rates in the ten auxiliary simulations of 100 revolutions also dropped to the same final value, which emerged as the lowest steady state power consumption observed across these simulations, one may infer that this final state is either the state of minimum dissipation or corresponds to a local minimum in configuration space.

Looking at the evolution in more detail, we notice that during the second decade of revolutions the system temporarily settles in a state with just slightly more dissipation than in the final stationary state. Curiously, in order to go from this intermediate state to the final state the system goes through a sequence of structures with dissipations almost as high as during the initial state. Moreover, there is a close resemblance between the evolution of the various contributions to the dissipation during this transition period and that during the initial period. Compare for example the evolution of the various contributions to the total dissipation between 2.5 and 12.5 revolutions with that between 30 and 42.5 revolutions. Surprisingly, during these periods, while the contributions of the small-large and large-large collisions to the total dissipation change substantially, their sum remains virtually constant.

We finally investigate where at the periphery of the system the power that is dissipated in the interior has been delivered. In fig. 6 we plot the various contributions to the delivered power at the various walls, as well as their final sum. We notice that most of the power is delivered at the cylindrical wall, and that the small amount of power delivered at the end-walls is more or less constant, independent of the actual type of particles present near these walls. Only during the later part of axial segregation and on the plateau in fig. 1 does the total consumed power decrease, mainly as a result of a decrease of the transfer of energy to the ever fewer large particles near the cylindrical wall. It is rather amazing that a temporary rise of the total dissipation to its initial level is finally followed by a decrease to a level slightly below its minimum up to that time. A similar behaviour has been found in shear banding systems [29,30] where the evolution of the total dissipation was non-monotonous in order to finally reach a level which was lower than any of its minima attained before.

In summary, we have been able to quantify the details of structural evolutions in a bed of granular particles after

starting to rotate the bed by using different measures of the entropy of the bed. The bed goes through a sequence of major conformational transitions, starting from an initially mixed state and passing through a radially segregated state before arriving at an axially segregated state, to repeat this sequence before settling in a final steady axially segregated state. Superimposed on the short-lived states of strong axial segregation, and to a lesser extent on the longer-lived states of weaker axial segregation, are rapid oscillations. These result from frictions with the end-walls that drag neighbouring particles along to higher angles of repose than in the center of the drum, followed by a dispersion of these particles toward the center of the drum. Moreover, we have found that the system eventually settles down in the state with the lowest energy dissipation rate of all traversed states, though the evolution to that state does not proceed by a monotonous decrease of the power consumption but by a two-stage process.

* * *

This work is supported with a grant of the Dutch Programme EET (Economy, Ecology, Technology), a joint initiative of the Ministries of Economic Affairs, Education, Culture and Sciences and of Housing, Spatial Planning and the Environment.

REFERENCES

[1] Das Gupta S., Khakhar D. V. and Bhatia S. K., *Powder Technol.*, **67** (1991) 145.
[2] Nakagawa M., Altobelli S. A., Caprihan A. and Fukushima E., *Chem. Eng. Sci.*, **52** (1997) 4423.
[3] Newey M., Ozik J., van der Meer S. M., Ott E. and Losert W., *Europhys. Lett.*, **66** (2004) 205.
[4] Taberlet N., Losert W. and Richard P., *Europhys. Lett.*, **68** (2004) 522.
[5] Nakagawa M., *Chem. Eng. Sci.*, **49** (1994) 2540.
[6] Hill K. M., Caprihan A. and Kakalios J., *Phys. Rev. Lett.*, **78** (1997) 50.
[7] Fiedor S. J. and Ottino J. M., *Phys. Rev. Lett.*, **91** (2003) 244301.
[8] Taberlet N., Newey M., Richard P. and Losert W., *J. Stat. Mech.*, **7** (2006) 7013.
[9] Alexander A., Muzzio F. J. and Shinbrot T., *Granular Matter*, **5** (2004) 171.
[10] Rapaport D. C., *Phys. Rev. E*, **65** (2002) 061306.
[11] Chicharro R., Peralta-Fabi R. and Velasco R. M., *Powders Grains*, **97** (1997) 479.
[12] Khan Z. S., Tokaruk W. A. and Morris S. W., *Europhys. Lett.*, **66** (2004) 212.
[13] Hill K. M. and Kakalios J., *Phys. Rev. E*, **52** (1995) 4393.
[14] Cundall P. A. and Strack O. D. L., *Geotechnique*, **29** (1997) 47.
[15] Schäfer J., Dippel S. and Wolf D. E., *J. Phys. I*, **6** (1996) 5.
[16] Arntz M. M. H. D., den Otter W. K., Briels W. J., Bussmann P. J. T., Beeftink H. H. and Boom R. M., *AIChE J.*, **54** (2008) 3313.
[17] Choo K., Baker M. W., Molteno T. C. A. and Morris S. W., *Phys. Rev. E*, **58** (1998) 6115.
[18] Choo K., Molteno T. C. A. and Morris S. W., *Phys. Rev. Lett.*, **79** (1997) 2975.
[19] Pohlman N. A., Ottino J. M. and Lueptow R. M., *Phys. Rev. E*, **74** (2006) 031305.
[20] Batchelor G. K., *An Introduction to Fluid Dynamics* (University Press Cambridge, Cambridge) 2002.
[21] Kim S. and Karrila S. J., *Microhydrodynamics. Principles and Selected Applications* (Butterworth-Heinemann, Stoneham, Mass.) 1991.
[22] Glansdorff P. and Prigogine I., *Thermodynamic Theory of Structure Stability and Fluctuations* (John Wiley & Sons Ltd, London) 1971.
[23] Martyushev L. M. and Seleznev V. D., *Phys. Rep.*, **426** (2006) 1.
[24] Onsager L., *Phys. Rev.*, **37** (1931) 405.
[25] Kohler M., *Z. Phys.*, **124** (1948) 212.
[26] Ziegler H., *An Introduction to Thermomechanics* (North-Holland Publishing Co., Amsterdam) 1977.
[27] Strutt J. W. (Lord Rayleigh), *Proc. London Math. Soc.*, **4** (1873) 357.
[28] Öttinger H. C., *Beyond Equilibrium Thermodynamics* (Wiley-Interscience, Hoboken) 2005.
[29] van den Noort A. and Briels W. J., *J. Non-Newton. Fluid Mech.*, **152** (2008) 148.
[30] van den Noort A. and Briels W. J., *Macromol. Theor. Simul.*, **16** (2007) 742.